



# Optical surface plasmon resonance sensor modified by mutant glucose/galactose-binding protein for affinity detection of glucose molecules

DACHAO LI,<sup>1</sup> JIE SU,<sup>1</sup> JIA YANG,<sup>2</sup> SONGLIN YU,<sup>2</sup> JINGXIN ZHANG,<sup>1</sup> KEXIN XU,<sup>1</sup> AND HAIXIA YU<sup>1,\*</sup>

<sup>1</sup>School of Precision Instrument and Opto-Electronics Engineering at Tianjin University, Tianjin 300072, China

<sup>2</sup>Tianjin Institute of Metrological Supervision and Testing, Tianjin 300192, China

\*hxy2081@tju.edu.cn

**Abstract:** Transdermal extraction of interstitial fluid (ISF) offers an attractive method for minimally invasive blood glucose monitoring. However, only a minute volume of ISF could be transdermally extracted, which is required to be diluted to form a manipulable volume of fluid for easy collection, transportation, and glucose detection. Therefore, a high-resolution glucose detection method is required for detecting glucose concentration in diluted ISF. In this paper, an optical surface plasmon resonance (SPR) sensor modified by the glucose/galactose-binding (GGB) protein which has good affinity to glucose molecules was presented for specific and sensitive glucose detection. The GGB protein was mutated at different sites for thiol coupling with the SPR surface and adjusting the affinity between glucose molecules and GGB protein. And the immobilization process of the GGB protein onto the surface of SPR sensor was optimized. Then, the stability of the SPR sensor modified with GGB protein was tested immediately and two weeks after immobilization. The coefficient of variation for glucose concentration measurement was less than 4.5%. By further mutation of the GGB protein at the A213S and L238S sites, the measurement range of the SPR sensor was adjusted to 0.1-100 mg/dL, which matches the glucose concentration range of 5-10 times diluted ISF (3-100 mg/dL). These results suggest that the SPR biosensor immobilized with GGB protein has the potential for continuous glucose monitoring by integrating into the microfluidic ISF extraction chip.

© 2017 Optical Society of America

**OCIS codes:** (240.6680) Surface plasmons; (130.6010) Sensors; (040.1880) Detection; (170.1420) Biology.

## References and links

1. T. Koutny, "Modelling of glucose dynamics for diabetes," in *Bioinformatics and Biomedical Engineering: 5th International Work-Conference*, I. Rojas and F. Ortuño, ed. (Springer, 2017), pp. 314–324.
2. L. McGahan, "Continuous glucose monitoring in the management of diabetes mellitus," *Issues Emerg. Health Technol.* **1–4**(32), 1–4 (2002).
3. C. Zecchin, A. Facchinetti, G. Sparacino, G. D. Nicolao, and C. Cobelli, "A new neural network approach for short-term glucose prediction using continuous glucose monitoring time-series and meal information," in *Proceedings of IEEE Conference on Engineering in Medicine and Biology Society* (IEEE, 2011), pp. 5653–5656.
4. P. Domachuk, M. Hunter, R. Batorsky, M. Cronin-Golomb, F. Omenetto, A. Wang, A. K. George, and J. C. Knight, "A path for non-invasive glucose detection using mid-IR supercontinuum," in *Proceedings of IEEE Conference on Quantum Electronics and Laser Science* (IEEE, 2008), pp. 1–2.
5. L. Malinin, "Development of a non-invasive blood glucose monitor based on impedance measurements," *Int. J. Biomed. Eng. Technol.* **8**(1), 60–81 (2012).
6. M. S. Talary, F. Dewarrat, D. Huber, L. Falco-Jonasson, and A. Caduff, "Non-invasive impedance based continuous glucose monitoring system," in *Proceedings of 13th International Conference on Electrical Bioimpedance and the 8th Conference on Electrical Impedance Tomography, Graz, Austria*, ed. (Springer, 2007), pp. 636–639.
7. R. Baghbani, M. A. Rad, and A. Pourziad, "Microwave sensor for non-invasive glucose measurements design and implementation of a novel linear," *IET Wirel. Sens. Syst.* **5**(2), 51–57 (2015).

8. R. J. Buford, E. C. Green, and M. J. McClung, "A microwave frequency sensor for non-invasive blood-glucose measurement," in *Proceedings of IEEE Conference on Sensors Applications Symposium* (IEEE, 2008), pp. 4–7.
9. N. Jahangiri, A. Bahrapour, and M. Taraz, "Non-invasive optical techniques for determination of blood glucose levels: A Review Article," *Iran. J. Med. Phys.* **11**(2), 224–232 (2014).
10. N. Tsuruoka, K. Ishii, T. Matsunaga, R. Nagatomi, and Y. Haga, "Lactate and glucose measurement in subepidermal tissue using minimally invasive microperfusion needle," *Biomed. Microdevices* **18**(1), 19 (2016).
11. G. Wang, M. D. Poscente, S. S. Park, C. N. Andrews, O. Yadid-Pecht, and M. P. Mintchev, "Minimally invasive pseudo-continuous blood glucose monitoring: results from in-vitro and in-vivo testing of the e-mosquito," in *Proceedings of IEEE International Symposium on Circuits and Systems* (IEEE, 2016), pp. 321–324.
12. J. J. Mastrototaro, K. W. Cooper, G. Soundararajan, J. B. Sanders, and R. V. Shah, "Clinical experience with an integrated continuous glucose sensor/insulin pump platform: A feasibility study," *Adv. Ther.* **23**(5), 725–732 (2006).
13. J. Mastrototaro, J. Shin, A. Marcus, and G. Sulur, STAR 1 Clinical Trial Investigators, "The accuracy and efficacy of real-time continuous glucose monitoring sensor in patients with type 1 diabetes," *Diabetes Technol. Ther.* **10**(5), 385–390 (2008).
14. R. L. Weinstein, S. L. Schwartz, R. L. Brazg, J. R. Bugler, T. A. Peyser, and G. V. McGarraugh, "Accuracy of the 5-day freestyle navigator continuous glucose monitoring system: comparison with frequent laboratory reference measurements," *Diabetes Care* **30**(5), 1125–1130 (2007).
15. D. M. Wilson, R. W. Beck, W. V. Tamborlane, M. J. Dontchev, C. Kollman, P. Chase, L. A. Fox, K. J. Ruedy, E. Tsalikian, and S. A. Weinzimer; DirecNet Study Group, "The accuracy of the freestyle navigator continuous glucose monitoring system in children with type 1 diabetes," *Diabetes Care* **30**(1), 59–64 (2007).
16. N. Wisniewski, F. Moussy, and W. M. Reichert, "Characterization of implantable biosensor membrane biofouling," *Fresenius J. Anal. Chem.* **366**(6-7), 611–621 (2000).
17. N. Wisniewski and M. Reichert, "Methods for reducing biosensor membrane biofouling," *Colloids Surf. B Biointerfaces* **18**(3-4), 197–219 (2000).
18. C. Sun, Y. Niu, F. Tong, C. Mao, X. Huang, B. Zhao, and J. Shen, "Preparation of novel electrochemical glucose biosensors for whole blood based on antibiofouling polyurethane-heparin nanoparticles," *Electrochim. Acta* **97**, 349–356 (2013).
19. D. A. Gough, J. Y. Lucisano, and P. H. Tse, "Two-dimensional enzyme electrode sensor for glucose," *Anal. Chem.* **57**(12), 2351–2357 (1985).
20. M. D. Raicopol, C. Andronescu, R. Atasiei, A. Hanganu, E. Vasile, A. M. Brezoiu, and L. Pilan, "Organic layers via aryl diazonium electrochemistry: towards modifying platinum electrodes for interference free glucose biosensors," *Electrochim. Acta* **206**, 226–237 (2016).
21. J. Kojima, S. Hosoya, C. Suminaka, N. Hori, and T. Sato, "An integrated glucose sensor with an all-solid-state sodium ion-selective electrode for a minimally invasive glucose monitoring system," *Micromachines (Basel)* **6**(7), 831–841 (2015).
22. K. Y. Hwa, B. Subramani, P. W. Chang, M. Chien, and J. T. Huang, "Transdermal microneedle array-based sensor for real time continuous glucose monitoring," *Int. J. Electrochem. Sci.* **10**(3), 2455–2466 (2015).
23. F. Ribet, G. Stemme, and N. Roxhed, "Ultra-miniaturization of a planar amperometric sensor targeting continuous intradermal glucose monitoring," *Biosens. Bioelectron.* **90**, 577–583 (2017).
24. M. J. Tierney, J. A. Tamada, R. O. Potts, L. Jovanovic, S. Garg, Cygnus Research Team, "Clinical evaluation of the GlucoWatch biographer: a continual, non-invasive glucose monitor for patients with diabetes," *Biosens. Bioelectron.* **16**(9-12), 621–629 (2001).
25. S. Mitragotri, M. Coleman, J. Kost, and R. Langer, "Transdermal extraction of analytes using low-frequency ultrasound," *Pharm. Res.* **17**(4), 466–470 (2000).
26. A. Jina, M. J. Tierney, J. A. Tamada, S. McGill, S. Desai, B. Chua, A. Chang, and M. Christiansen, "Design, development, and evaluation of a novel microneedle array-based continuous glucose monitor," *J. Diabetes Sci. Technol.* **8**(3), 483–487 (2014).
27. H. Yu, D. Li, R. C. Roberts, K. Xu, and N. C. Tien, "An interstitial fluid transdermal extraction system for continuous glucose monitoring," *J. Microelectromech. Syst.* **21**(4), 917–925 (2012).
28. H. Vaisocherová, H. Šípová, I. Višová, M. Bocková, T. Špringer, M. L. Ermini, X. Song, Z. Krejčík, L. Chrastinová, O. Pastva, K. Pimková, M. Dostálová Merkerová, J. E. Dyr, and J. Homola, "Rapid and sensitive detection of multiple microRNAs in cell lysate by low-fouling surface plasmon resonance biosensor," *Biosens. Bioelectron.* **70**, 226–231 (2015).
29. R. P. Liang, G. H. Yao, L. X. Fan, and J. D. Qiu, "Magnetic Fe<sub>3</sub>O<sub>4</sub>@Au composite-enhanced surface plasmon resonance for ultrasensitive detection of magnetic nanoparticle-enriched  $\alpha$ -fetoprotein," *Anal. Chim. Acta* **737**, 22–28 (2012).
30. R. Ballerstadt and J. S. Schultz, "Kinetics of dissolution of Concanavalin A/Dextran sols in response to glucose measured by surface plasmon resonance," *Sens. Actuators B Chem.* **46**(1), 50–55 (1998).
31. J. W. Mannhalter, D. G. Gilliland, and R. J. Collier, "A hybrid toxin containing fragment A from diphtheria toxin linked to the B protomer of cholera toxin," *Biochim. Biophys. Acta* **626**(2), 443–450 (1980).
32. D. Li, D. Yang, J. Yang, Y. Lin, Y. Sun, H. Yu, and K. Xu, "Glucose affinity measurement by surface plasmon resonance with borate polymer binding," *Sens. Actuators A Phys.* **222**, 58–66 (2015).

33. M. N. Vyas, N. K. Vyas, and F. A. Quijoch, "Crystallographic Analysis of the Epimeric and Anomeric Specificity of the Periplasmic Transport/Chemosensory Protein Receptor for D-Glucose and D-Galactose," *Biochemistry* **33**(16), 4762–4768 (1994).
34. D. M. Miller 3rd, J. S. Olson, and F. A. Quijoch, "The mechanism of sugar binding to the periplasmic receptor for galactose chemotaxis and transport in *Escherichia coli*," *J. Biol. Chem.* **255**(6), 2465–2471 (1980).
35. N. K. Vyas, M. N. Vyas, and F. A. Quijoch, "Sugar and signal-transducer binding sites of the *Escherichia coli* galactose chemoreceptor protein," *Science* **242**(4883), 1290–1295 (1988).
36. N. K. Vyas, M. N. Vyas, and F. A. Quijoch, "A novel calcium binding site in the galactose-binding protein of bacterial transport and chemotaxis," *Nature* **327**(6123), 635–638 (1987).
37. J. Y. Zou, M. M. Flocco, and S. L. Mowbray, "The 1.7 Å Refined X-ray Structure of the Periplasmic Glucose/Galactose Receptor from *Salmonella typhimurium*," *J. Mol. Biol.* **233**(4), 739–752 (1993).
38. K. Weidemaier, A. Lastovich, S. Keith, J. B. Pitner, M. Sistare, R. Jacobson, and D. Kurisko, "Multi-day pre-clinical demonstration of glucose/galactose binding protein-based fiber optic sensor," *Biosens. Bioelectron.* **26**(10), 4117–4123 (2011).
39. H. V. Hsieh, D. B. Sherman, S. A. Andaluz, T. J. Amiss, and J. B. Pitner, "Fluorescence resonance energy transfer glucose sensor from site-specific dual labeling of glucose/galactose binding protein using ligand protection," *J. Diabetes Sci. Technol.* **6**(6), 1286–1295 (2012).
40. A. V. Nashchekin, O. A. Usov, and K. K. Turoverov, "Waveguide-type localized plasmon resonance biosensor for noninvasive glucose concentration detection," *Proc. SPIE* **8427**, 842739 (2012).
41. T. J. Amiss, D. B. Sherman, C. M. Nycz, S. A. Andaluz, and J. B. Pitner, "Engineering and rapid selection of a low-affinity glucose/galactose-binding protein for a glucose biosensor," *Protein Sci.* **16**(11), 2350–2359 (2007).
42. H. V. Hsieh, Z. A. Pfeiffer, T. J. Amiss, D. B. Sherman, and J. B. Pitner, "Direct detection of glucose by surface plasmon resonance with bacterial glucose/galactose-binding protein," *Biosens. Bioelectron.* **19**(7), 653–660 (2004).
43. P. A. Berntsson, "Structure and function of substrate-binding proteins of ABC-transporters," University of Groningen (2010).
44. S. Núñez, J. Venhorst, and C. G. Kruse, "Target-drug interactions: first principles and their application to drug discovery," *Drug Discov. Today* **17**(1-2), 10–22 (2012).

## 1. Introduction

Diabetes mellitus is a common disease that threatens human health, and it is important to monitor the blood glucose of diabetics continuously for diagnosis and treatment [1–3]. Among the existing detection methods, invasive methods are not suitable for dynamic and continuous glucose monitoring due to the pain of blood sampling. Meanwhile, the non-invasive method based on optics [4], impedance [5, 6] and microwave detection [7, 8] is far from clinical application because of low signal-noise ratio and weak specificity [9]. Therefore, the minimally-invasive blood glucose monitoring technology, which has promising future in clinic application, has become the research hotspot in recent years [10, 11]. For minimally-invasive method, the glucose concentration in interstitial fluid (ISF) could be measured for blood glucose concentration prediction either by implantable sensors or ISF transdermal extraction.

The enzyme electrode, as an implantable sensor, is utilized to measure the enzyme reaction electricity while the enzyme electrode is implanted into subcutaneous tissue. The representative products based on this technique include SEVEN® Plus (DexCom, Inc.) [12], Paradigm REAL-Time (Medtronic, Inc.) [13, 14], FreeStyle Navigator (Abbott Laboratories) [15], etc. However, there are two main disadvantages of the enzyme electrode sensing technique. As an implanted biosensor, the biofouling of electrode surface can be developed by the proteins and other biological matter. And the biofouling of electrode surface will bring catastrophic damage to the electron transfer between enzyme and electrode redox center [16–18]. In addition, many endogenous electroactive species such as ascorbic and uric acids, as well as drugs (e.g. paracetamol) can be easily oxidized at the applied potential. The contribution from various electroactive species present in biological fluids severely compromises the selectivity and accuracy of glucose monitoring [19, 20]. Therefore, it's still a challenge for continuous glucose monitoring.

Contrary to the above-mentioned techniques, transdermal extraction of ISF offers an attractive method for minimally-invasive blood glucose monitoring [21–23]. The methods of ISF transdermal extraction can be diverse: reverse iontophoresis [24], ultrasonic penetration [25], and hollow microneedle arrays [26]. Our group [27] implemented the low-frequency

ultrasound for increasing the skin permeability and ISF was transdermally extracted with higher fluxes as vacuum was applied to enhance the convection of ISF. And then, a minute volume of ISF, which scattered on the skin surface in the form of droplets, need to be diluted to form a manipulable volume of fluid for easy collection and transportation based on a microfluidic chip. Since the ISF was diluted, it's very important to develop a high-resolution method for detecting glucose concentration at low level.

Surface plasmon resonance (SPR) technology is an optical high-resolution detection method for biomolecules [28, 29]. However, SPR sensor cannot detect glucose molecules specifically, as it measures the change of refractive index on the surface of gold film. All components in ISF can contribute to the change of refractive index on the sensor surface. Therefore, the biochemical modification on the surface of gold film is required for specific detection of glucose molecules in ISF. The effective molecules modified on the SPR sensor surface for glucose detection include Concanavalin A (ConA), glucose/galactose-binding (GGB) protein and borate polymer. Ballerstadt and Schultz [30] designed a SPR modified with a droplet of highly viscous sol consisting of ConA and dextran. They detected glucose concentration at 0-50 mM. But it is only a preliminary measurement indicated feasibility of glucose detection based on this method. In addition, since ConA is toxic [31], it is not suitable for detecting glucose concentration in the ISF. The borate polymer PAA-ran-PAAPBA was modified on the SPR sensor surface for the quantitation of glucose concentration by Li and Yang [32]. The measurement resolution of sensor bound to 12 polymer layers was 1 mg/dL and the detection range was 1-1000 mg/dL. However, the resolution is not good at the low level of glucose concentration (1-10 mg/dL,  $R^2 = 0.78823$ ), which is important for detecting glucose in the diluted ISF.

In this paper, GGB protein was chosen to modify the surface of gold film on the prism SPR sensor. As GGB protein has good affinity to glucose molecules, the glucose molecules in the ISF with complex components could be specifically detected. The immobilized GGB protein exists in a solid state on the surface of SPR sensor and it is able to associate and disassociate with the glucose molecules dynamically. In addition, via the mutations at different sites of GGB protein, different ranges of glucose concentration can be detected accurately, which makes the detection of glucose concentration in ISF at different dilution ratios possible. Thus, this developed SPR sensor integrated with the microfluidic ISF extraction chip which has been studying in our lab [27] presents a simple and stable platform toward sensitive and minimally-invasive glucose detection, which has great potential to monitor glucose continuously for the management of diabetes.

## 2. Surface modifications of SPR sensor by mutant GGB protein

### 2.1 Characterization and preparation of GGB protein and mutant GGB protein

GGB protein was found as the primary high-affinity receptor of active transport for and chemotaxis toward glucose and galactose in the periplasm of bacterial cells. Furthermore, the affinity of GGB protein for glucose, determined by equilibrium and reaction kinetics, is 2-fold tighter than for galactose [33]. This is reflected in the results of ligand-binding competition studies [34] and structure determination [35] which showed that GGB protein as purified, has bound endogenous glucose exclusively.

The GGB protein is a monomer of 32 kDa consisting of two main folded domains, the N-terminus domain and the C-terminus domain. The two domains are connected by a flexible hinge portion consisting of three peptide chains. The hinge portion can bend to an angle of at least  $18^\circ$  and open a gap to show the glucose binding sites. When the glucose molecules are absorbed to the binding sites, the two folded domains of GGB protein come closer because of the change in the hinge portion, leading to a variation in the spatial conformation of GGB protein eventually [36-40]. Thus, the combination of GGB protein and glucose molecule has a high degree of specificity and affinity.

Based on the above characterization, the genetically mutant GGB protein which is more suitable for bio-sensing of glucose was prepared for the immobilization on the SPR sensor surface for specific glucose detection. E149C, A213S, and L238S were introduced to the GGB protein by site mutation. These mutated sites were proposed for two purposes. Firstly, cysteine which has the mercapto group (-SH) was introduced to E149C by target site mutation to realize GGB protein immobilization by thiol coupling. Secondly, as the natural GGB protein would be saturated at large glucose concentrations [41, 42], polar amino acids were introduced to replace intrinsically hydrophobic amino acids at the A213S and L238S sites for reducing the affinity between GGB protein and glucose molecule to obtain wider detection range of glucose concentrations.

Preparation of the mutant GGB protein includes five main steps. Initially, the mutation at the predetermined gene point was completed. The second step was constructing the mutant type of engineering bacteria. And then, the cells were harvested by culturing engineering bacteria. Furthermore, the periplasmic protein was extracted by osmotic shock method. Finally, the GGB protein was purified by Ni-NTA purification technology. The above five steps were developed and performed by cooperation with School of Chemical Engineering and Technology of Tianjin University.

## 2.2 Immobilization of mutant GGB protein

The mutant GGB protein was immobilized onto the gold surface of SPR sensor by self-assembling method (SAM), as shown in Fig. 1(a). The structure is similar to a sandwich, where A, B, C, D and E represent the prism, the gold film, the self-assembled layer, GGB protein and glucose molecules, respectively. When glucose solutions with different concentrations are flowed through the sensor surface, mutant GGB protein can absorb the glucose molecules specifically, causing the change of surface refractive index by which glucose concentration is derived.

Mutant GGB protein was immobilized to the SPR sensor chip using the thiol coupling method (Fig. 1(b)). The experiments were carried out using an SPR instrument (BIAcore 3000, GE) with a sensor chip which has a layer of dextran on its surface (CM5). There is a temperature control module in the instrument and all experiments were carried out at 25 °C. The sample flow rate was set at 5  $\mu\text{L}/\text{min}$  except for special instructions.

Firstly, the gold surface of SPR sensor was immersed into the mixture of 0.4 M EDC (1-(3-dimethylaminopropyl)-3-ethylcarbodiimide hydrochloride) and 0.1 M NHS (N-hydroxymaleimide) at the volume ratio of 1:1 for 7 minutes to activate the monolayer. And the residue of EDC/NHS was removed by flowing PBS (pH 7.4, 0.01 M) for 2min. And then, PDEA (Poly N, N-diethylacrylamide, 80 mM) was injected to the sensor surface for 4 min to form disulfide. The residue of PDEA was also removed by flowing PBS. After that, GGB protein solution (40  $\mu\text{g}/\text{mL}$ ) was flowed through the surface for 10min with the residual GGB protein removal by PBS. At last, the cysteine/NaCl solution was flowed through the surface for 2 min to deactivate the residual active position. After successful immobilizing, the surface was washed with PBS for a period of time, which is benefit to gain a stable binding surface. The response curve of SPR sensor was detected in the GGB protein immobilization process, as shown in Fig. 1(c).

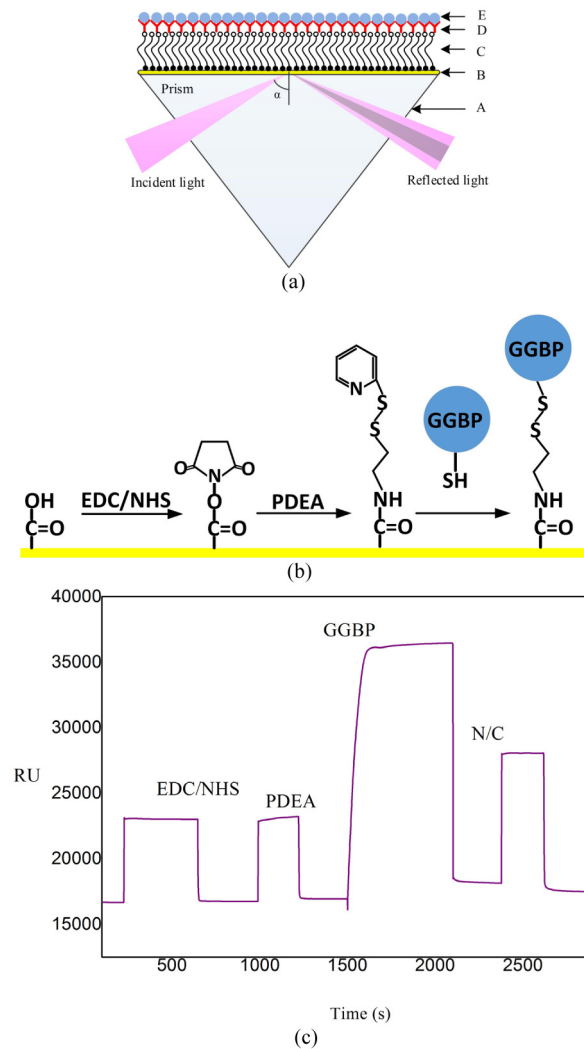


Fig. 1. (a) The SAM structure of the SPR-gold surface. A, B, C, D and E represent the prism, the gold film, the self-assembled layer, GGB protein and glucose molecules, respectively. (b) Immobilization process of GGB protein on the gold surface of SPR sensor chip. (c) The response curve of GGB protein immobilization process.

## 2.3 Optimization of mutant GGB protein immobilization conditions

### 2.3.1 Influence of pH value

The protein can be either positively charged or negatively charged while dissolving in buffer solution with different pH values. Notably, when the positive charge is equal to the negative charge, this pH value is called the isoelectric point (PI) of the protein. When the pH value of the buffer solution is lower than the PI, the protein is positively charged, while on the contrary, it is negatively charged. The PI of GGB protein is 5.7 [43]. Thus, the protein is positively charged when the pH value of the buffer solution is lower than 5.7. Furthermore, when the pH value of the buffer solution is higher than 3.5, the carboxylate dextran on the CM5 chip is negatively charged. Therefore, if the pH value of the buffer solution is between 3.5 and 5.7, the charge of the protein is opposite to that of the sensor surface, and they can be

adsorbed with each other. The influence of pH on the affinity between the sensor surface and protein is shown in Fig. 2.

Based on the above principle, the sodium acetate buffers at pH 4.0, 4.5, 5.0, 5.5 were chosen to dissolve triple sites mutant GGB protein to the final concentration of 40  $\mu\text{g/mL}$ . These four GGB protein solutions were injected to the sensor surface respectively, and the response curves are shown in Fig. 3. The maximum response of about 20000  $\Delta\text{RU}$  was obtained when the pH value of buffer was 4.5, which showed the best attracting ability between the GGB protein and sensor surface. Then the protein immobilization process introduced in section 2.2 was carried out using the GGB protein solutions except the solution dissolved with the buffer at pH 5.5. After the successful immobilization, the PBS was flowed through the sensor surface, and the response values of the three SPR sensors immobilized with different GGB protein solutions were shown in Fig. 4. The maximum response of 1200  $\Delta\text{RU}$  was obtained from the SPR sensor which was immobilized with the GGB protein dissolved in the buffer at pH 4.5, which means this sensor has the largest density of immobilized GGB protein on the sensor surface and best binding effect. Therefore, the buffer at pH 4.5 was used to dissolve GGB protein in the following experiments.

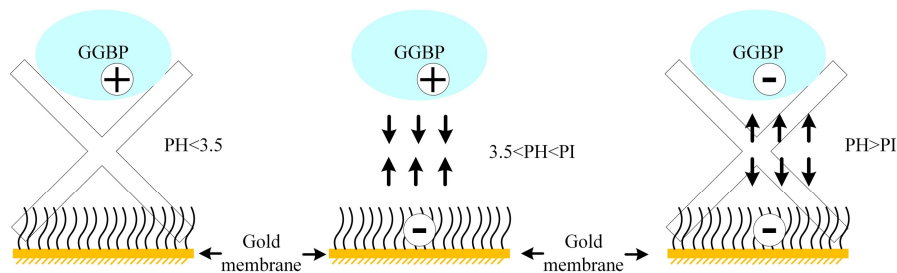


Fig. 2. Influence of pH on the affinity between the surface and protein

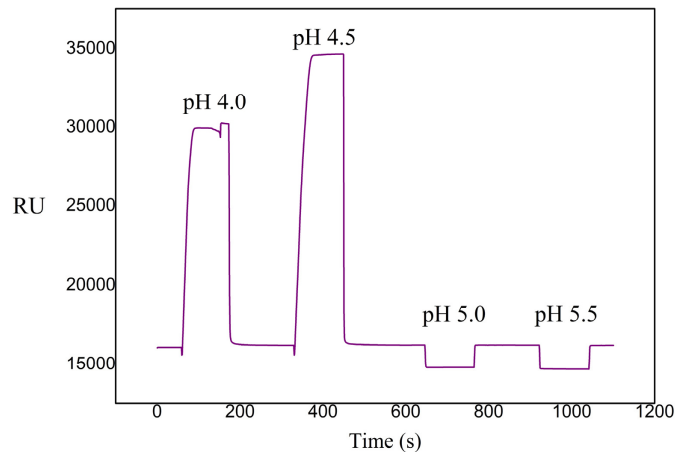


Fig. 3. Response of GGB protein at different pH values.

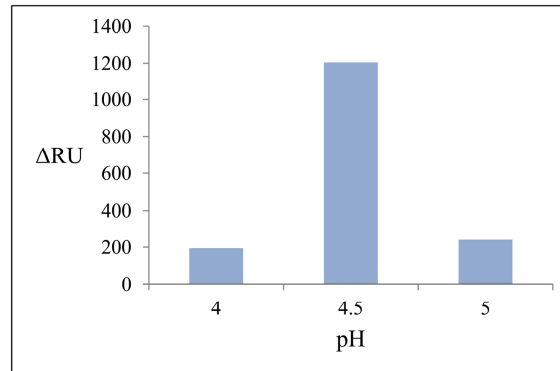


Fig. 4. Influence of pH values on protein binding effect.

### 2.3.2 Influence of GGB protein concentration

The triple sites mutant GGB protein solutions with the concentrations of 20  $\mu\text{g/mL}$ , 40  $\mu\text{g/mL}$ , 80  $\mu\text{g/mL}$ , and 100  $\mu\text{g/mL}$  were tested to analyze the influence of GGB protein concentration on protein immobilization efficiency. Firstly, the GGB protein solutions were injected to the sensor surface and the response curves are shown in Fig. 5. The maximum response of about 20000  $\Delta RU$  was obtained when the concentration was 40  $\mu\text{g/mL}$ , which showed the best affinity between the sensor surface and GGB protein. Then the protein immobilization process introduced in section 2.2 was implemented using the GGB protein solutions at 20  $\mu\text{g/mL}$ , 40  $\mu\text{g/mL}$ , 60  $\mu\text{g/mL}$ . The maximum response of 1200  $\Delta RU$  was obtained from the SPR sensor which was immobilized with the GGB protein solution at 40  $\mu\text{g/mL}$ , which means this sensor has the largest density of immobilized GGB protein on the sensor surface and best binding effect (Fig. 6). Therefore, the GGB protein solution at 40  $\mu\text{g/mL}$  was used in the following experiments.

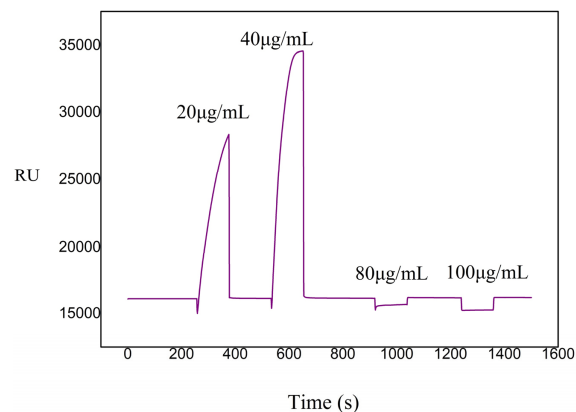


Fig. 5. Response of different GGB protein concentrations.



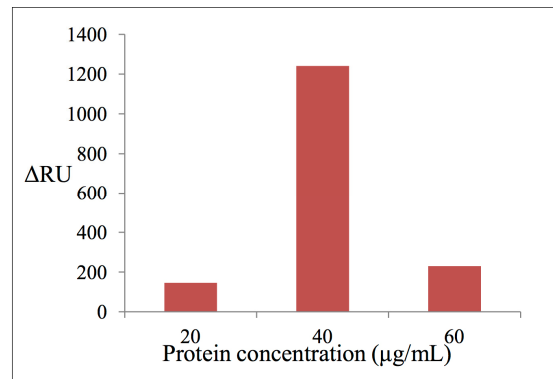


Fig. 6. Influence of protein concentrations on binding effect.

#### 2.4 Regeneration of SPR sensor

The measurements of glucose solutions were performed in direct succession, with no regeneration process between each sample in one measurement cycle. The immobilized GGB protein exists in a solid state on the surface of SPR sensor and it is able to associate and disassociate with the glucose molecules dynamically [44]. During glucose solution injection, the glucose molecules bind to the surface-attached GGB protein, resulting in an increase in signal and reaching a steady state. When the glucose solution is replaced by a continuous flow of buffer, the corresponding decrease in signal reflects dissociation of glucose molecules from the GGB protein. After that, the SPR sensor is ready for the next measurement of glucose solution.

After one measurement cycle, alkaline solution was injected to flow through the sensor surface for regenerating the sensor and the self-assembled layer remained. The mutant GGB protein can be immobilized on the regenerated sensor surface by thiol coupling again. The regenerated sensor can repeatedly be used up to eluting the self-assembled layer.

### 3. Glucose detection by modified SPR sensor

In order to achieve higher detection accuracy, the GGB protein immobilization parameters, such as pH value and the concentration of GGB protein, were firstly tested and optimized. Under the optimal immobilization conditions, two kinds of mutant GGB protein, the single site mutant protein (E149C) and the triple sites mutant protein (E149C, A213S, L238S), were immobilized to the sensor surface respectively. Both of the sensors were tested in solutions with different glucose concentrations for satisfying the range of glucose concentration in diluted ISF, which was carried out on the BIAcore 3000. The experiments were carried out at 25 °C and the sample flow rate was set at 5 μL/min.

#### 3.1 Glucose detection by single site mutant GGB protein

Under optimal immobilization conditions, single site (E149C) mutant GGB protein was immobilized on the SPR sensor surface by thiol coupling (as introduced in section 2.2). And then, glucose solutions with different concentrations were tested using the sensor to analyze and evaluate its performance. To eliminate the interference of temperature fluctuation and system drift, the PBS solution as a reference sample was flowed through the SPR sensor surface before each glucose detection. Then the measured refractive indexes of the PBS solution and the following glucose solution formed a data pair to calculate the difference of refractive index which reflected the glucose concentration. In the experiment, seven glucose solutions were prepared using PBS as a solute, and their glucose concentrations were in the range of 0.1-10 mg/dL (as shown in Table 1). Each glucose solution was tested three times in

the aforementioned process, and the difference of refractive index for each measurement was shown in Table 1. In addition, the averaged results are shown in Fig. 7. The linear fitting curve between the difference of refractive index and glucose concentration indicates their good correlation.

**Table 1. Measurements of glucose concentrations using SPR sensor immobilized with single site mutant GGB protein**

| Glucose concentrations(mg/dL) | First group | Second group | Third group | Average |
|-------------------------------|-------------|--------------|-------------|---------|
| 0.10                          | 19.7        | 17.9         | 21.4        | 19.7    |
| 0.25                          | 20.9        | 21.3         | 23.1        | 21.7    |
| 0.50                          | 22.7        | 18.1         | 20.8        | 20.5    |
| 1.00                          | 35.1        | 28.1         | 26.5        | 29.9    |
| 2.50                          | 49.0        | 50.1         | 42.9        | 47.3    |
| 5.00                          | 42.4        | 54.7         | 53.4        | 50.2    |
| 10.0                          | 113         | 116          | 110         | 113     |

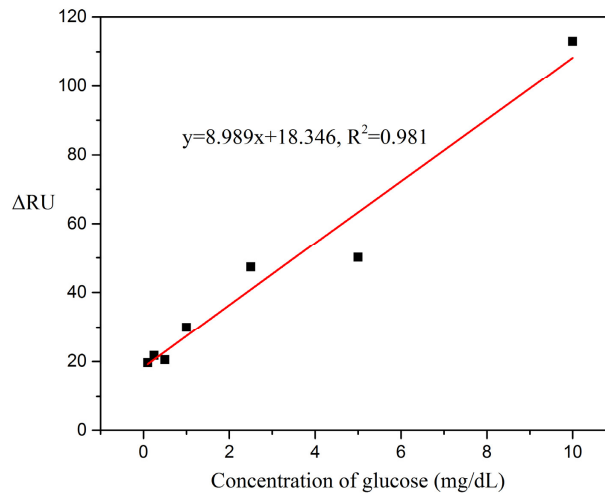


Fig. 7. Linear fitting curve between the difference of refractive index and glucose concentration.

In order to verify the repeatability of the SPR sensor immobilized with GGB protein, a glucose solution of 0.5 mg/dL was tested eight times following the process introduced in the above paragraph. After that, the sensor was immersed in 4° C PBS for two weeks. And then, a glucose solution of 5 mg/dL was tested eight times in the same process. As shown in Table 2, the measured differences of refractive index for glucose solutions of 0.5 mg/dL and 5 mg/dL were  $27.6 \pm 1.18$  RU and  $52.8 \pm 0.37$  RU, respectively. And the coefficient of variation was lower than 4.5%. The SPR sensor immobilized with GGB protein is stable for glucose measurement not only just after immobilization, but also after immersing in 4° C PBS for two weeks.

**Table 2. The measured differences of refractive index for glucose solutions (unit: RU)**

| Glucose concentration | 1    | 2    | 3    | 4    | 5    | 6    | 7    | 8    | Average | Standard deviation | Coefficient of variation |
|-----------------------|------|------|------|------|------|------|------|------|---------|--------------------|--------------------------|
| 0.5 mg/dL             | 25.6 | 26.4 | 27.0 | 27.4 | 28.0 | 28.7 | 29.2 | 28.8 | 27.6    | 1.18               | 4.28%                    |
| 5.0 mg/dL             | 52.1 | 52.2 | 52.9 | 53.2 | 52.8 | 52.9 | 52.9 | 53.1 | 52.8    | 0.37               | 0.70%                    |

### 3.2 Glucose detection by triple sites mutant GGB protein

In general, the measurement range of home use glucometer is 30-500 mg/dL, while the SPR sensor immobilized single site mutant GGB protein can only detect the glucose solution at 0.1-10 mg/dL accurately. In order to detect glucose concentration in the diluted ISF at the dilution ratio of 5-10 times (3-100 mg/dL), it is necessary to expand the detection range based on SPR sensor by adjusting the affinity between GGB protein and glucose molecule. Therefore, apart from single site mutant at the E149C site, A213S and L238S were introduced to enlarge detection range of glucose concentration as introduced in section 2.1.

Under optimal immobilization conditions, a triple site (E149C, A213S, L238S) mutant GGB protein was immobilized on the SPR sensor surface by thiol coupling (as introduced in section 2.2). In the experiment, glucose solutions in three concentration ranges were prepared using PBS as a solute. The three ranges were 0.1-1 mg/dL ( $\Delta = 0.2$  mg/dL), 1-10 mg/dL ( $\Delta = 1$  mg/dL), and 10-100 mg/dL ( $\Delta = 10$  mg/dL), respectively. Each glucose solution was tested following the process introduced in section 3.1. The experimental data were fit to a quadratic curve, and the results are shown in Fig. 8(a)-8(c). The R-square of the fitting curve are 0.97, 0.91 and 0.91 respectively at the concentration ranges of 0.1-1 mg/dL, 1-10 mg/dL and 10-100 mg/dL, which indicate good correlation between the glucose concentration and SPR signal. Thus, the detection range of the SPR sensor immobilized with triple sites mutant GGB protein is 0.1-100 mg/dL which covers the range of glucose concentration (3-100 mg/dL) in ISF at the dilution ratio of 5-10.

The small plateaus in  $\Delta$ RU at some concentrations (0.3 mg/dL, 1-6 mg/dL, 10-20 mg/dL) were caused by the instrument drift when changing the settings of instrument. To verify the validity of detecting glucose solution at different concentrations, three concentration ranges (0.1-1 mg/dL, 1-10 mg/dL, 10-100 mg/dL) were detected based on SPR sensor modified with triple sites mutant GGB protein and the intervals of the three ranges ( $\Delta = 0.2$  mg/dL,  $\Delta = 1$  mg/dL,  $\Delta = 10$  mg/dL) were different. While changing different intervals of glucose concentration, the settings of instrument were switched artificially, which has a negative effect on the SPR signal at the beginning of experiments. Despite existing this phenomenon, the experimental results have shown the validity of measurements, and this phenomenon cannot appear in the practical application for continuous glucose monitoring. But the solution to this phenomenon will be found in the next step.

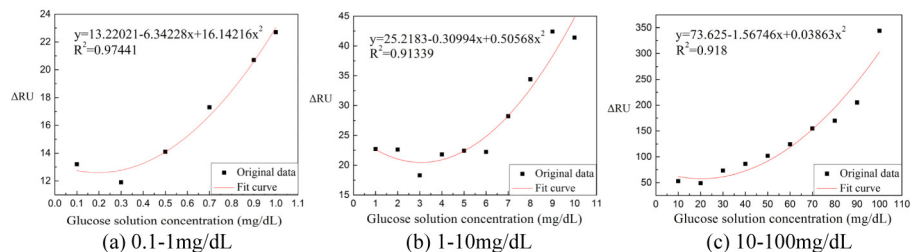


Fig. 8. Fitting curve between the difference of refractive index and glucose concentration.

#### 4. Conclusions

The main contribution of this paper was developing an optical SPR sensor modified with mutant GGB protein for high resolution glucose detection with low concentration, which can be potentially applied to detect glucose concentration in diluted ISF. Two kinds of GGB protein were synthesized by mutation at different sites. One was mutated at the E149C site, and the other was mutated at triple sites (E149C, A213S and L238S). Both mutant GGB proteins were immobilized onto sensor surface by thiol coupling as cysteine was introduced at the E149C site. For the triple sites mutant GGB protein, the mutation at the A213S and L238S sites was used for satisfying the range of glucose concentration in diluted ISF. As a result, the SPR sensor immobilized with the triple sites mutant GGB protein could accurately detect the glucose concentration in the range of 0.1-100 mg/dL, which fulfills the requirement for glucose detection in 5-10 times diluted ISF (3-100 mg/dL). This developed high-resolution strategy of detecting glucose concentration at the low level can also be applied to many commercial SPR sensors. For continuous glucose monitoring as a wearable device, the small sensor which integrated the light source and detector (e.g., spreeta sensor, Texas Instruments) is proposed to integrate with a microfluidic ISF extraction chip, and a disposable cheap PBS solution tube will be provided with patients for ISF dilution and glucose detection in one day.

#### Funding

National Natural Science Foundation of China (81571766, 61428402); the Key Projects of Tianjin Natural Science Foundation Program (15JCZDJC36100); the Key Projects in the Science & Technology Pillar Program of Tianjin (11ZCKFSY01500); the Natural Science Foundation of Tianjin (17JCYBJC244 00); the 111 Project of China (B07014).

#### Acknowledgments

The authors acknowledge Prof. Rui Ban's Group from the School of Chemical Engineering and Technology in Tianjin University for their contributions to the GGB protein synthesis.

#### Disclosures

The authors declare that there are no conflicts of interest related to this article.